Graph Models of Electric Power Transmission Networks Using Synchrophasor Data

Ganesh K. Venayagamoorthy, *Fellow, IEEE*, Dulip Madurasinghe, *Graduate Student Member, IEEE*,
Rajan Ratnakumar, *Graduate Student Member, IEEE*
Real-Time Power and Intelligent Systems Laboratory
Department of Electrical and Computer Engineering, Clemson University, SC 29634, USA
gkumar@ieee.org, dtmadurasinghe@ieee.org, rajan94@ieee.org

***Abstract*—The electric power transmission network (EPTN) is a connected, geographically distributed network, which can be represented with a graph model with nodes and edges. The graph represents the physical connectivity of the EPTN. Deriving the graph model of the EPTN solely based on continually measured data is important for reliable power system operational situation awareness and decreasing uncertainties driven by weather, electrification, and interconnections. In this paper, an exhaustive search algorithm is presented to derive the EPTN graph model (TNGM) solely based on synchrophasor measurements retrieved from the substations without prior knowledge of the connectivity. Furthermore, an evaluation metric for any data-driven TNGM is introduced. The transmission network of the two-area, four-machine power system is used as the test system, and typical TNGMs for different power plant operating conditions are presented. Typical graphs obtained for network impedance and power flows are shown to be accurate, on average within 2% error margin.**

***Index Terms*—Impedance graph, power flow graph, synchrophasor data, graph construction, transmission network**

I. Introduction

The electric power system is considered the most critical infrastructure today due to the dependency of other critical infrastructures on it such as communication, gas, health, military, transportation and water. Thus, the reliability and security of the electric power transmission network (EPTN) is paramount. Furthermore, the electric power grid modernization is rapidly transforming the EPTN to meet the needs of the increasing demand patterns and new generation sources. The EPTN is the backbone of the power system that connects large-scale generation with the load centers. Reliable delivery of bulk power depends on secure EPTN operation. An accurate and near real-time understanding of the connectivity of the large geographically distributed EPTN is crucial for optimum power transmission, routing and quick emergency restoration with EPTN reconfiguration [1]. State-of-the-art (SOTA) EPTN connectivity understanding is based on the breaker status communicated through relays to the energy control center (ECC) via supervisory control and data acquisition (SCADA), which is used to establish the EPTN topology (TNT). The efficiency (SCADA can only deliver measurement at around 2-6 s [2]), accuracy, reliability and security of SCADA communications has shortcomings for modern power system operations [3].

Introducing the phasor measurement units (PMUs) to the EPTN has enabled new ways to improve power system monitoring and control. A PMU measures bus voltage phasor and branch current phasors at 30 Hz and higher sampling rates (up to 240 Hz), and the system frequency and rate of change of frequency is computed [4]. The time-tagged phasor measurements are transmitted to a Phasor Data Concentrator (PDC) [5]. The synchronized measurements of a geographically distributed EPTN is useful for ECC data analytics and decision-making.

There has been previous and current ongoing research efforts to enhance the SOTA TNT. TNT using fuzzy c-means algorithm with power and current flows is proposed in [6]. Near real-time TNT based on new circuit breaker monitoring architecture is proposed in [7]. A data-driven hierarchical TNT process is proposed in [8]. In these proposed methods and the SOTA, prior knowledge of network connectivity is required to complete the procedure.

In this paper, a transmission network graph model (TNGM) derivation from solely PMU measurements transmitted to an ECC without any prior understanding of the network connectivity is presented. The proposed approach utilizes an exhaustive search algorithm based on the physics of the power system (power flows and impedances) to identify the accurate matches of sending and receiving power flows. The TNGM can be useful for providing redundancy for the SOTA TNT, validation of the SOTA TNT and an alternative approach to provide alerts on false-data injection attacks. The overview of the proposed approach is shown in Fig. 1. The resulting matched power flow pairs are used to construct the TNGM. Furthermore, based on the constructed TNGM, two graphs can be derived, namely a network impedance graph to depict the impedance of each branch in the transmission network and a power flow graph to provide the power flows in the transmission network.

The rest of the paper is organized as follows: Section II introduces the power system graph models, including network impedance and power flow graphs. Section III describes the proposed data-driven graph modeling method. Typical results and discussions are presented in Section IV. Section V provides a conclusion on the findings and future work.

This work was supported by the National Science Foundation (NSF) of the United States, under grants CNS 2131070, ECCS 2234032 and CNS 2318612. Any opinions, findings and conclusions or recommendations expressed in this material are those of author(s) and do not necessarily reflect the views of NSF.

SoutheastCon 2024 | 979-8-3503-1710-7/24/$31.00 ©2024 IEEE | DOI: 10.1109/SOUTHEASTCON52093.2024.10500111

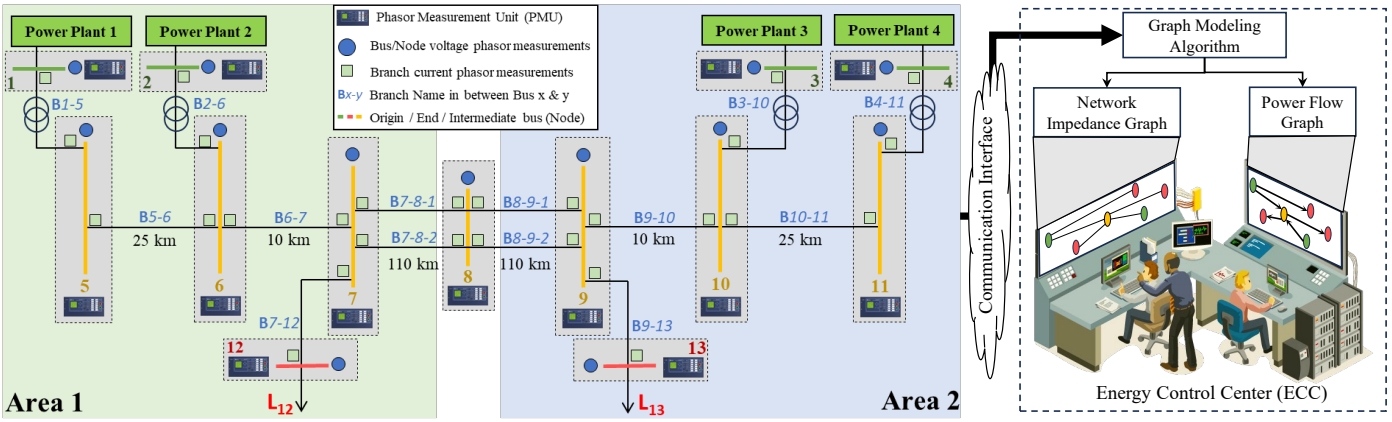

Fig. 1. Data-driven graph modeling of electric power transmission networks.

II. Power System Graph Models

A power system transmission network is a geographically distributed interconnected system. Thus, the physical connectivity of the transmission network can be represented with a graph. The nodes and edges in a graph represent the buses and branches in a electric power transmission network, respectively.

A. Power System

The EPTN considered in this study is from the Kundur's two-area four-machine power system model [9]. The power system diagram is depicted in Fig. 1, which has 13 buses and 14 branches.This two-area, four-machine symmetrical system has in each area, five buses (Area 1: 1, 2, 5, 6, 7 and Area 2: 3, 4, 9, 10, 11) and two power plants (PPs) (Area 1: PP 1, PP2 and Area 2: PP 3, PP 4). The two areas are connected by two tie-lines (a double transmission line with an intermediate bus (bus 8). Two zero-impedance branches (B7-12 and B9-13) exist to connect the load buses (12 and 13). All transmission lines (B5-6, B6-7, B7-8-1, B7-8-2, B8-9-1, B8-9-2, B9-10, B10-11) have $0.0001 + j0.001$ per units (pu) impedance per kilometer. There is a phasor measurement unit (PMU) installed at each bus for measuring its voltage phasor and branch current phasors of the branches connected to it at 30 Hz [4].

B. Transmission Network Graph Models

The TNGMs have nodes (buses) and edges (branches). The nodes can be either end (generation or load feeders) or intermediate nodes. The intermediate nodes enable EPTN reconfiguration and control. Fig. 2 classifies all possible types of nodes in TNGM based on the different types of buses that can be found in an EPTN. The two TNGMs that be derived for an EPTN are described below.

1) Network Impedance Graph: The network impedance graph of the EPTN, a non-directed graph, depicts the characteristic impedance of each transmission branch. The network impedance graph representation can be constructed using the derived TNGM. The network impedance graph is a static graph where the edge values (characteristic impedance) do not change

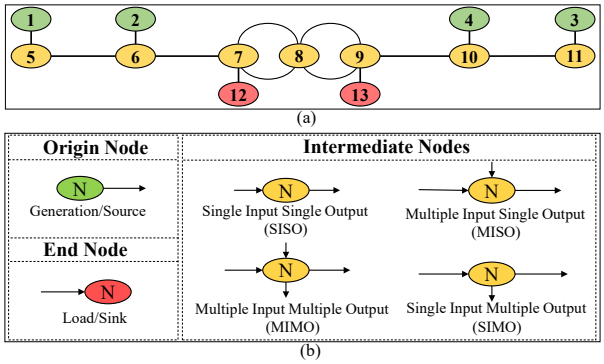

Fig. 2. (a) Transmission network graph model (TNGM) of the Kundur's power system shown Fig. 1 based on prior knowledge. (b) The six types of nodes that can be found in a TNGM

under different operating conditions of the EPTN for a given TNGM.

2) Power Flow Graph: The power flow graph of the EPTN is a directed graph that presents the direction power flows, inflows and outflows at a bus. The graph derivation procedure described in Section III-B1 is based on the fundamental principles of power transfer over a transmission line. In each transmission branch, the power flow at the sending end should be equal to the sum of the power flow at the receiving end and the power loss in the transmission line. The power flow graph can be constructed from the derived TNGM and directly correlated to the ECC's SOTA power flow analysis tool in the energy management system (EMS). The power flow graph is a dynamic graph where the edge values (power flows) can change under different operating conditions of the EPTN.

III. Data-Driven Graph Modeling

The PMUs are increasingly implemented on the EPTN due to their operational advantages. The PMUs are capable of transmitting synchronized phasor quantities, such as bus voltages and branch currents, at higher rates than with SCADA. Circuit nodal analysis is carried out at each EPTN bus utilizing the bus (nodes) voltage phasor measurements and branch (edges)

current phasor measurements collected from PMUs. The bus voltage and branch current phasor quantities can be used to estimate network branch power flows and impedances. This caters for rule-based exhaustive searches to be applied to find the best match of receiving and sending end power flows for each branch. EPTN bus connectivity can be established since each branch power flow is with respect to measurements at a given bus.

A. Synchrophasor Mesurements and Data Format

One or more PMUs are installed at every EPTN bus to collect voltage and current phasors in a generic data format. It is important to note that the objective of this study is to derive the EPTN connectivity in form of a graph model without any prior knowledge but solely based on PMU data. Thus, every bus is assumed to be a single graph node without any known connectivity. The PMU at every bus is tagged with a unique identification and the respective PMU measurements are tagged with the same identification. Thus, a generic data format is established as follows. w is an assigned Bus (PMU) identification number, x is the variable identifier, y is the number of measurement of a particular variable, and z is the measurement type (magnitude or angle). Since there is one voltage measurement from each bus, the voltage measurement is designated with "V_1" variable identifier. For example, the magnitude and angle measurements of the voltage phasor of Bus '12' variable names according to this naming convention are "BUS_12_V_1_mag" and "BUS_12_V_1_ang", respectively. The current phasor measurements always start with "I_1" and ends up with "I_h", where is h is the total number of branches at a given bus. For example, the magnitude and angle measurements of the 'fourth' current phasor quantity of the Bus '8' variable name by this convention are "BUS_8_I_4_mag" and "BUS_8_I_4_ang", respectively. A snapshot of one PMU sample in the data file is shown in Table. A.1. The phasor measurements are shown for voltage magnitudes are in volts (V), current magnitudes in amperes (A), and voltage and current angles angles in radians.

B. Graph Construction

1) Procedure: The exhaustive search process for constructing a graph model of an EPTN is shown in Figs. 3 and 4. It starts by importing measurements from all the PMUs in an EPTN following the naming convention described above, in Section III-A. Then, for each bus, all active power flows (P) are calculated using (1) with their voltage and current phasor measurements, where $|V|$ refers to the bus voltage magnitude, $|I|$ refers to the branch current magnitude, θ refers to the bus voltage angle and α refers to the branch current angle.

$$P(i) = 3|V||I|cos(\theta + (-\alpha)) \tag{1}$$

After all power flows (inflows and outflows from buses) are computed, the values are stored with bus identification (ID) numbers, w. With an exhaustive search for each $bus\ i$ (as shown in Fig. 3) with potential matching power flow (j), the best match of an inflow bus is identified for given outflow bus or vice-versa. The following filtration (selection) step is carried out based on the fundamentals of power flow between two buses. For a branch between two buses, the power inflow (at the sending-end) should be matched as close as possible (accounting for transmission loss) with the outflow (at the receiving-end) or vice versa. Thus, all power outflows from other buses are filtered out if the selected power flow is an outflow or vice versa. After this filtration step, the filtered candidate power flows are added to the candidate list of power flows to be matched with power flow j.

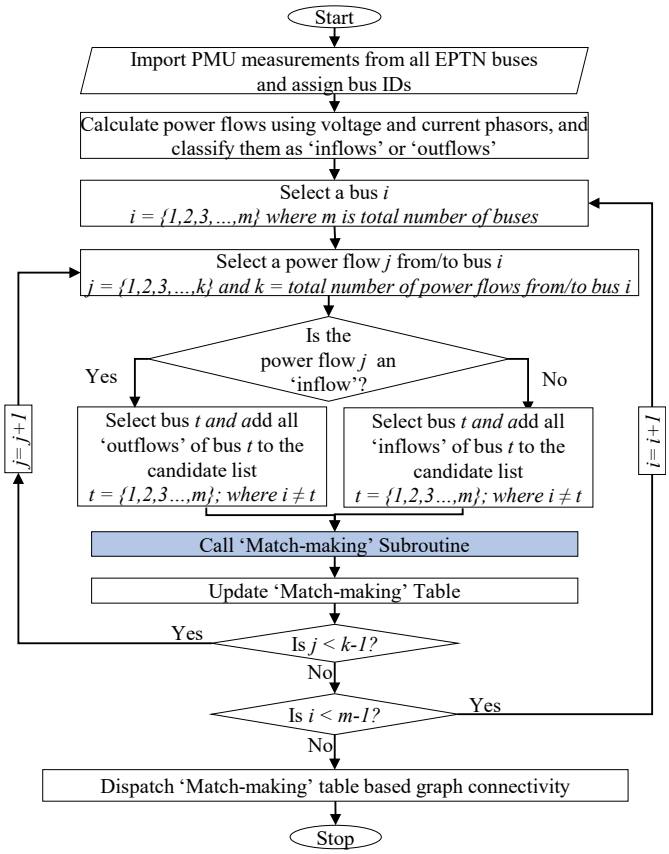

Fig. 3. A flowchart for construction of an TNGM based on exhaustive search using synchrophasor data.

The "Match-making" subroutine is executed for the candidate list of power flows filtered from the above stated branch power flow fundamentals . In this subroutine, all candidates are individually analyzed. Out of all the candidate power flows, a candidate r is selected to match with power flow j. The current flow should be identical in a given branch at either ends, sending and receiving. In practice, the sending end current should be close to the receiving end current measurement. Given that the current phasor measurements are available for all candidate flows, the absolute branch-ends current flow difference ($ACFD$) can be calculated using the current magnitudes of $I(r)$ and $I(j)$, using (2). If the $ACFD$ exceeds a small percentage threshold ΔI_{TH}, the candidate r is dropped from

the candidate list.

$$ACFD_{r,j} = ||I(r)| - |I(j)|| \tag{2}$$

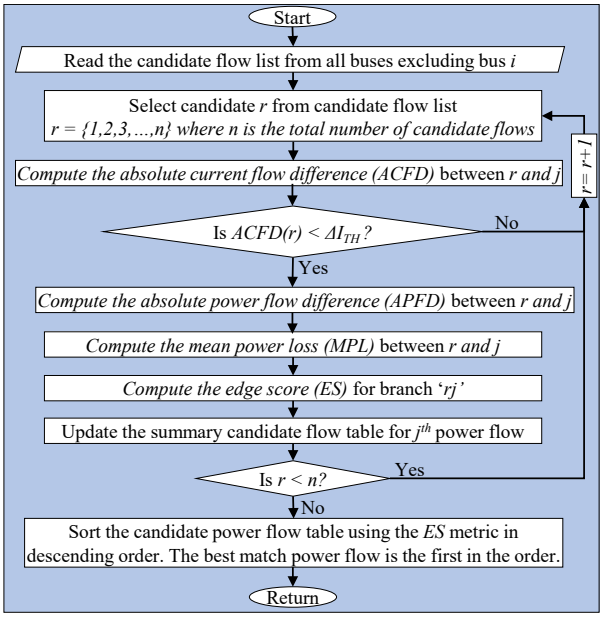

Fig. 4. Subroutine for match-making of EPTN buses for the TNGM construction based on the fundamentals of power transfer over a transmission line.

The exhaustive search is continued from the above-reduced candidate list based on the $ACFD$ calculations. There is an active power loss for any power transfer over a transmission lines. This power loss can be calculated using two independent methods. Since all power flows at all the buses are available, a simple calculation of an absolute power flow difference ($APFD$) between the active powers, $P(r)$ and $P(j)$, can be computed as shown in (3). On the other hand, the mean power loss (MPL) can be computed using (4) and (5) for each possible candidate branch. Theoretically, if a branch connects with between buses r and j, the $APFD_{r,j}$ should be equal to the $MPL_{r,j}$. However, in practice, there can be a small difference. Based on that, an edge score (ES) value is calculated using (6) by simply taking the inverse of the absolute difference of $APFD$ and MPL with a very small constant, c, added to avoid an infinity error.

$$APFDr, j = ||P(r)| - |P(j)|| \tag{3}$$

$$I\_mean_{r,j} = \frac{(I_r \angle \alpha_r) + (I_j \angle \alpha_j)}{2} \tag{4}$$

$$MPL_{r,j} = |Real((V_r \angle \theta_r) - (V_j \angle \theta_j) * (I\_mean_{r,j})^*)| \tag{5}$$

$$ES_{r,j} = \frac{1}{|APFD_{r,j} - MPL_{r,j}| + c} \tag{6}$$

Finally, the best match is selected by the top candidate in the ES scores,sorted in a descending order of all candidates in the reduced list.

2) TNGM Validity and Score: The exhaustive search procedure explained above in Section III-B1 generates a best match table, where all bus ID-tagged branch flows are matched, resulting in a TNGM. The ES concept can be extended to develop a metric for evaluating $TNGM$ score derived from other search methods. The $TNGM$ score is a generic metric to evaluate other possible $TNGM$ and to determine the best TNGM that represents the connectivity of a given EPTN. For a given TNGM, the ES can be calculated for every branch using (6) and then $TNGM$ score can be computed using (7). The assumption made in this paper is that PMUs are installed on all buses of the EPTN and their measurements are available for construction of TNGMs. The total number of current measurements from all the PMUs in the EPTN is twice the number of branches present in the EPTN since each branch current is measured at the sending and receiving ends. Given this, "Rule 1" - the number of edges in a TNGM should be half of the number of PMU current flow measurements obtained for a EPTN - is established to classify generated TNGMs as valid (feasible) graph representations or invalid ones. Furthermore, the lower the $TNGM$ score, the better the graph representation of the connectivity in a EPTN. A TNGM that is one-to-one with the connectivity of the EPTN will have the lowest $TNGM$ score.

$$TNGMscore = \begin{cases} \sum_{i=1}^{Edges} \frac{1}{ES(i)}; & \text{if "Rule 1" satisfy} \\ invalid; & \text{otherwise} \end{cases} \tag{7}$$

IV. Results and Discussion

The two-area four-machine power system model shown in Fig. 1 [9] is simulated on the real-time digital simulator (RTDS). Three different operating conditions depicted in Table III are studied in this paper. The network impedance and power flow graphs generated for these three power plant operating conditions are presented and discussed in Sections IV-A and IV-B, respectively. The match-making table resulting from an exhaustive search is depicted in Table I for the three power plant operating conditions. It is to be noted that power flow matches in double circuit lines (B7-8-1 with B7-8-2 and B8-9-1 with B8-9-2) is indifferent since identical bus and line characteristics result in identical flows in both circuit lines. Such conditions do not affect TNGM generated.

A. Network Impedance Graph

The TNGMs for network impedance graph based on a single set of PMU measurements of the EPTN in steady-state for three different operating conditions are shown in Fig. 5. The impedance is denoted in per-unit (pu) with a base impedance of 528.99 ohms. In the study for this paper, seven buses (excluding load and generator buses) and eight branches (excluding generator-transformer branches and zero impedance

TABLE I
THE MATCH-MAKING RESULTS WITH THE POWER FLOWS IDS FOR THREE DIFFERENT POWER PLANT OPERATING CONDITIONS.

Power Flow Name	Flow ID	True Match Flow ID	Search Match Flow ID		
			High	Medium	Low
PP1 (SE)	1	5	5	5	5
PP2 (SE)	2	7	7	7	7
PP3 (SE)	3	26	26	26	26
PP4 (SE)	4	23	23	23	23
PP1 (RE)	5	1	1	1	1
B5-6 (SE)	6	8	8	8	8
PP2 (RE)	7	2	2	2	2
B5-6 (RE)	8	6	6	6	6
B6-7 (SE)	9	10	10	10	10
B6-7 (RE)	10	9	9	9	9
B7-12 (SE)	11	27	27	27	27
B7-8-1 (SE)	12	14	15	15	15
B7-8-2 (SE)	13	15	15	15	15
B7-8-1 (RE)	14	12	13	13	12
B7-8-2 (RE)	15	13	13	13	12
B8-9-1 (SE)	16	18	19	19	19
B8-9-2 (SE)	17	19	19	19	19
B8-9-1 (RE)	18	16	16	16	16
B8-9-2 (RE)	19	17	16	16	16
B10-9 (RE)	20	22	22	22	22
B9-13 (SE)	21	28	28	28	28
B10-9 (SE)	22	20	20	20	20
PP4 (RE)	23	4	4	4	4
B11-10 (RE)	24	25	25	25	25
B11-10 (SE)	25	24	24	24	24
PP3 (RE)	26	3	3	3	3
B7-12 (RE)	27	11	11	11	11
B9-13 (RE)	28	21	21	21	21

load branches) of the two-area four-machine power system are represented by the TNGM.

Furthermore, the two end-currents of a branch may not be exactly the same in practice, thus, the branch impedance is computed based on mean current flow (given by (4)) using (8).

$$Z_{r,j} = \frac{(V_r \angle \theta_r) - (V_j \angle \theta_j)}{I\_mean_{r,j}} \tag{8}$$

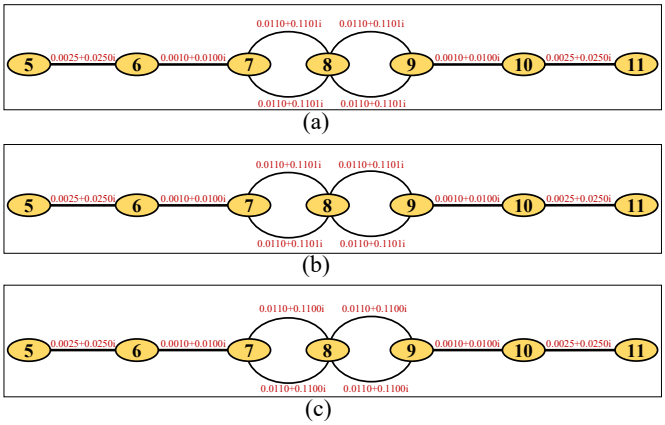

Fig. 5. TNGMs depicting branch impedances (in pu) for three different power plant operating conditions. (a) High, (b) Medium and (c) Low. The network impedance graphs are identical for different power plant operating conditions.

B. Power Flow Graph

The TNGMs for power flow based on a single set of PMU measurements of the EPTN in steady-state for three different operating conditions are shown in Fig. 6. For this study, all 13 buses and 14 branches of the two-area four-machine power system are considered.

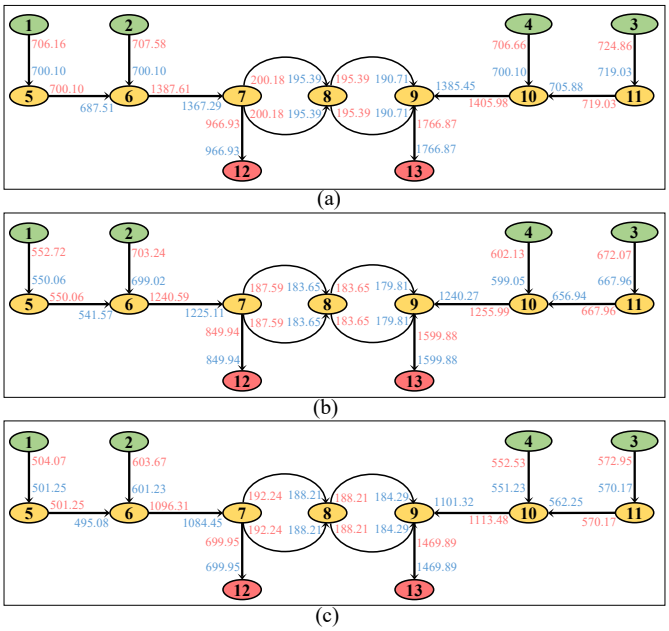

Fig. 6. TNGMs depicting active power flows (in MWs) for three different power plant operating conditions. (a) High, (b) Medium and (c) Low.

C. Discussion

The comparison of the impedance values ('Ground Truth') used in the RTDS EPTN simulation model and branch impedances in TNGMs obtained from the synchrophasor data are shown in Table II. The comparison is based on one-minute of PMU measurement data (1800 samples) for the EPTN under steady-state. Based on the error analysis, the obtained TNGMs for network impedances for the three different power plant operating conditions are similar to the ground truth values used in the RTDS simulation model.

The comparison of the power flows in TNGMs (shown in Fig. 6) have been compared with the power flow values obtained from the RTDS simulation model. This is depicted in Table III. As can be observed, the values are similar for the three different power plant operating conditions.

V. CONCLUSION

The construction of a transmission network graph model solely from synchrophasor measurement data obtained from electric power transmission network has been presented in this paper. The TNGM, representing the physical connectivity of the EPTN, is important for monitoring, control and optimization in modern power systems. For practical applications in energy control centers, the TNGMs will provide system operators with

TABLE II
COMPARISON OF TNGM NETWORK IMPEDANCE VALUES WITH THE GROUND TRUTH VALUES FOR THREE DIFFERENT POWER PLANT OPERATING CONDITIONS.

Branch	Ground Truth Impedance (pu)	Impedance Errors in Percentage (%)					
		High		Medium		Low	
		Real	Imaginary	Real	Imaginary	Real	Imaginary
B5-6	0.0025+ 0.0250i	1.72± 4.89E-15	0.01± 6.85E-17	1.72± 6.89E-15	0.01± 6.94E-18	1.72± 1.44E-15	9.1E-04± 2.65E-18
B6-7	0.0010+ 0.0100i	0.01± 1.04E-16	0.01± 2.60E-17	0.01± 7.63E-17	0.01± 1.51E-16	0.01± 5.38E-17	2.1E-03± 1.99E-17
B7-8-1	0.0110+ 0.1100i	0.42± 2.17E-15	0.08± 9.30E-16	0.31± 1.33E-15	0.06± 5.55E-17	0.30± 1.83E-15	0.04± 3.82E-16
B7-8-2	0.0110+ 0.1100i	0.42± 2.05E-15	0.08± 9.72E-17	0.31± 1.11E-15	0.06± 2.64E-16	0.30± 2.05E-15	0.04± 1.53E-16
B8-9-1	0.0110+ 0.1100i	0.12± 1.17E-15	0.08± 1.96E-16	0.02± 3.47E-17	0.06± 1.04E-16	0.01± 1.13E-16	0.04± 3.89E-16
B8-9-2	0.0110+ 0.1100i	0.12± 1.18E-15	0.08± 1.74E-16	0.02± 9.37E-17	0.06± 3.61E-16	0.01± 2.95E-17	0.04± 1.53E-16
B9-10	0.0010+ 0.0100i	0.01± 1.91E-17	0.01± 4.69E-17	0.01± 1.21E-17	0.01± 6.59E-17	0.01± 4.69E-17	2.1E-03± 3.27E-18
B10-11	0.0025+ 0.0250i	1.72± 1.99E-15	0.01± 7.45E-17	1.72± 2.67E-15	0.01± 3.75E-18	1.72± 4.22E-15	8.1E-04± 5.69E-18

TABLE III
COMPARISON OF ACTIVE POWER FLOW VALUES OF THE TNGMS WITH THAT OF THE RTDS SIMULATION MODEL FOR THREE DIFFERENT POWER PLANT OPERATING CONDITIONS.

Generation/ Load/ Branches	Active Power (MW)					
	Measured (Ground Truth) in MWs			Percentage Error from Ground Truth (%)		
	High	Medium	Low	High	Medium	Low
PP 1	700.2	549.1	501.3	0.88± 8.46E-05	0.49± 8.46E-05	0.81± 8.43E-05
PP 2	700.2	699.1	601.3	1.08± 8.43E-0.5	0.46± 8.52E-05	0.61± 8.35E-05
PP 3	719.1	668.0	570.2	0.67± 8.51E-05	0.31± 8.39E-05	0.52± 8.43E-05
PP 4	700.2	599.1	551.3	0.95± 8.51E-05	0.35± 8.50E-05	0.46± 8.41E-05
B5-6	700.1	549.1	201.3	1.46± 8.59E-05	1.68± 8.72E-05	2.29± 8.64E-05
B6-7	1388.0	1241.0	1096.0	0.17± 8.40E-05	0.05± 8.34E-05	0.58± 8.35E-05
B7-8	200.2	187.6	192.3	2.66± 8.62-05	1.95± 8.39E-05	2.26± 8.64E-05
B8-9	195.4	183.7	188.2	0.20± 8.31E-05	0.19± 8.38E-05	0.11± 8.47E-05
B9-10	1406.0	1256.0	1114.0	1.51± 8.55E-05	0.32± 8.36E-05	0.31± 8.28E-05
B10-11	719.1	668.0	570.2	1.27± 3.06E-05	1.20± 8.59E-05	1.81± 8.61E-05
Load 12	967.0	850.0	700.0	0.01± 8.35E-05	0.01± 8.12E-05	0.01± 8.38E-05
Load 13	1767.0	1600.0	1470.0	0.01± 8.36E-05	0.01± 8.41E-05	0.01± 8.46E-05

enhanced situational awareness. Different update frequency of the TNGMs can be provided to the system operators in ECCs as needed. Furthermore, an evaluation metric for TNGMs has been presented. This metric provides an awareness of how close the TNGM's representation is to the physical transmission line connectivity. The presented data-driven approach has been demonstrated and validated on the EPTN of the two-area four-machine power system. The network impedance and power flow graphs have been presented for three different power plant operating conditions. Given the nature of the presented data-driven approach, data integrity and availability are essential for reliability and dependence in ECCs. Future work includes incorporating generator-transformer branches, and investigating the approach for EPTN topology changes. More robust and fast search methods will be needed for larger EPTNs.

REFERENCES

[1] T. Aziz, Z. Lin, M. Waseem, and S. Liu, "Review on optimization methodologies in transmission network reconfiguration of power systems for grid resilience," *International Transactions on Electrical Energy Systems*, vol. 31, no. 3, p. e12704, 2021. [Online]. Available: https://onlinelibrary.wiley.com/doi/abs/10.1002/2050-7038.12704

[2] X. Kong, Y. Chen, T. Xu, C. Wang, C. Yong, P. Li, and L. Yu, "A hybrid state estimator based on scada and pmu measurements for medium voltage distribution system," *Applied Sciences*, vol. 8, no. 9, 2018. [Online]. Available: https://www.mdpi.com/2076-3417/8/9/1527

[3] M. Farrokhabadi and L. Vanfretti, "State-of-the-art of topology processors for ems and pmu applications and their limitations," in *IECON 2012 - 38th Annual Conference on IEEE Industrial Electronics Society*, Montreal, QC, Canada, 2012, pp. 1422–1427.

[4] J. De La Ree, V. Centeno, J. S. Thorp, and A. G. Phadke, "Synchronized phasor measurement applications in power systems," *IEEE Transactions on Smart Grid*, vol. 1, no. 1, pp. 20–27, June 2010.

[5] B. Appasani and D. K. Mohanta, "A review on synchrophasor communication system: communication technologies, standards and applications," *Protection and Control of Modern Power Systems*, vol. 3, no. 1, p. 37, Dec 2018. [Online]. Available: https://doi.org/10.1186/s41601-018-0110-4

[6] D. Singh, J. Pandey, and D. Chauhan, "Topology identification, bad data processing, and state estimation using fuzzy pattern matching," *IEEE Transactions on Power Systems*, vol. 20, no. 3, pp. 1570–1579, 2005.

[7] M. Kezunovic, "Monitoring of power system topology in real-time," in *Proceedings of the 39th Annual Hawaii International Conference on System Sciences (HICSS'06)*, Kauia, HI, USA, 2006, pp. 1–10.

[8] D. Madurasinghe and G. K. Venayagamoorthy, "An efficient and reliable electric power transmission network topology processing," *IEEE Access*, vol. 11, pp. 127 956–127 973, 2023.

[9] P. Kundur, "Power system stability and control," McGraw-Hill, 1994.

APPENDIX

TABLE A.1
SNAPSHOT OF DATA FILE (HIGH OPERATING CONDITION) USING THE DEFINED DATA NAMING CONVENTION.

Time	BUS_1_V_1_ang	BUS_1_V_1_mag	BUS_1_I_1_ang	BUS_1_I_1_mag	BUS_2_V_1_ang
0.0333	0.470856667	1.03078031	0.241555929	2.344946233	0.30049634
BUS_2_V_1_mag	BUS_2_I_1_ang	BUS_2_I_1_mag	BUS_3_V_1_ang	BUS_3_V_1_mag	BUS_3_I_1_ang
1.010746453	0.005179167	2.43912672	0	1.030784961	-0.210903883
BUS_3_I_1_mag	BUS_4_V_1_ang	BUS_4_V_1_mag	BUS_4_I_1_ang	BUS_4_I_1_mag	BUS_5_V_1_ang
2.397128999	-0.177757263	1.010754572	-0.430667877	2.407047019	0.881675124
BUS_5_V_1_mag	BUS_5_I_1_ang	BUS_5_I_1_mag	BUS_5_I_2_ang	BUS_5_I_2_mag	BUS_6_V_1_ang
1.006508844	0.765154839	2.344946133	0.736901522	2.343040674	0.705704331
BUS_6_V_1_mag	BUS_6_I_1_ang	BUS_6_I_1_mag	BUS_6_I_2_ang	BUS_6_I_2_mag	BUS_6_I_3_ang
0.978037906	0.528777838	2.43912677	3.872353554	2.343896712	0.613387108
BUS_6_I_3_mag	BUS_7_V_1_ang	BUS_7_V_1_mag	BUS_7_I_1_ang	BUS_7_I_1_mag	BUS_7_I_2_ang
4.749411358	0.558909178	0.960964616	3.753792405	4.749516722	0.455867767
BUS_7_I_2_mag	BUS_7_I_3_ang	BUS_7_I_3_mag	BUS_7_I_4_ang	BUS_7_I_4_mag	BUS_8_V_1_ang
3.371904768	0.529497147	0.694677485	0.529497147	0.694677485	0.317684174
BUS_8_V_1_mag	BUS_8_I_1_ang	BUS_8_I_1_mag	BUS_8_I_2_ang	BUS_8_I_2_mag	BUS_8_I_3_ang
0.948750422	3.583265841	0.691804544	3.583265841	0.691804625	0.441673279
BUS_8_I_3_mag	BUS_8_I_4_ang	BUS_8_I_4_mag	BUS_9_V_1_ang	BUS_9_V_1_mag	BUS_9_I_1_ang
0.691804544	0.441673279	0.691804625	0.081220389	0.971336682	3.495658517
BUS_9_I_1_mag	BUS_9_I_2_ang	BUS_9_I_2_mag	BUS_9_I_3_ang	BUS_9_I_3_mag	BUS_9_I_4_ang
0.679592902	3.495658517	0.679592983	3.3117342	4.773311389	0.024690151
BUS_9_I_4_mag	BUS_10_V_1_ang	BUS_10_V_1_mag	BUS_10_I_1_ang	BUS_10_I_1_mag	BUS_10_I_2_ang
6.073060936	0.228098631	0.983386261	0.171332598	4.773408972	0.092931032
BUS_10_I_2_mag	BUS_10_I_3_ang	BUS_10_I_3_mag	BUS_11_V_1_ang	BUS_11_V_1_mag	BUS_11_I_1_ang
2.407046957	3.419999957	2.3957027	0.407964707	1.008324674	0.284441948
BUS_11_I_1_mag	BUS_11_I_2_ang	BUS_11_I_2_mag	BUS_12_V_1_ang	BUS_12_V_1_mag	BUS_12_I_1_ang
2.395181718	0.312695026	2.397129	0.558909178	0.960964616	3.597460421
BUS_12_I_1_mag	BUS_13_V_1_ang	BUS_13_V_1_mag	BUS_13_I_1_ang	BUS_13_I_1_mag	
3.371904768	0.081220389	0.971336682	3.166282805	6.073060936	